

## A METHOD OF INCREASING THE ACCURACY OF LOW-STIFFNESS SHAFTS: SINGLE-PASS TRAVERSE GRINDING WITHOUT STEADY RESTS

Paweł SUŁKOWICZ<sup>\*</sup>, Robert BABIARZ<sup>\*</sup>, Jan BUREK<sup>\*</sup>, Jarosław BUK<sup>\*</sup>, Kamil GANCARCZYK<sup>\*</sup>

<sup>\*</sup>Faculty of Mechanical Engineering and Aeronautics, Rzeszow University of Technology,  
al. Powstańców Warszawy 12, 35-959 Rzeszów, Poland

[sulkowicz@prz.edu.pl](mailto:sulkowicz@prz.edu.pl), [robertb@prz.edu.pl](mailto:robertb@prz.edu.pl), [jburek@prz.edu.pl](mailto:jburek@prz.edu.pl), [jbuk@prz.edu.pl](mailto:jbuk@prz.edu.pl), [kamilgancarczyk@prz.edu.pl](mailto:kamilgancarczyk@prz.edu.pl)

*received 8 June 2022, revised 4 August 2022, accepted 12 August 2022*

**Abstract:** The article presents a method of increasing the shape and dimensional accuracy of low-stiffness shafts manufactured in a single pass of a grinding wheel in traverse grinding. One-pass manufacturing is one of the ways for reducing machining time and increasing efficiency, thus lowering production costs. However, maintaining the necessary accuracy proves to be a challenge because the whole machining allowance has to be removed at once, leaving no room for errors that could be fixed in additional passes of the tool. It is especially true in finishing operations, such as traverse grinding. In addition, grinding the workpiece in a single pass of a grinding wheel leads to high forces, which cause elastic deformation of the part. The lower the stiffness of the part, the more difficult it is to achieve the required accuracy. As a result, there are many methods of improving the accuracy of grinding such parts, but they tend to be either expensive or reduce the machining efficiency. Thus, it is important to seek new methods that would allow improving the accuracy of the machining without reducing its efficiency. The proposed method does not require using steady rests and is based on the measurement of the normal grinding force component. Knowing the value of the grinding force when grinding with a set grinding depth, the elastic deformation of the machine tool–tool–workpiece system is calculated in each position of the grinding wheel. Based on the calculated deformation, the additional infeed of the grinding wheel is implemented in order to stabilise real grinding depth and to increase the accuracy of the produced part. The experimental tests were conducted to prove the effectiveness of the proposed method.

**Key words:** traverse grinding, low-stiffness shafts, single-pass grinding, cylindricity error

### 1. INTRODUCTION

Grinding is a machining process traditionally used to achieve high accuracy and surface quality of the workpiece with low cutting volume. The developments in the field of abrasive materials as well as in the design and technological capabilities of modern grinding machines enable the implementation of many new processes and machining strategies. High-efficiency grinding (HEG) processes are used in order to reduce machining time and lower production costs. The methods that allow achieving such task are collectively named high-performance grinding (HPG) or HEG [1]. Two directions of the development in high-performance grinding processes can be distinguished, namely, deep grinding methods and grinding processes with high grinding wheel peripheral speeds. In the case of deep-cut grinding (DCG) processes, high machining efficiency is achieved as a result of using high values of grinding wheel infeed (grinding depth  $a_e$ ), relatively low feed rates of the workpiece and low peripheral speed of a grinding wheel. An alternative solution is to increase the peripheral speed of the grinding wheel, which, in turn, allows improving machining efficiency while maintaining the required surface quality due to a significant increase in grinding speed (e.g., high-speed grinding, HSG) [2–4]. Most high-performance grinding methods, however, are based not on increasing the grinding speed but on the use of high grinding depth values in many cases, allowing the workpiece to be machined with a single pass of a grinding wheel [5].

There are three main grinding processes that can be executed in a single pass of a grinding wheel. The first one is the creep feed grinding (CFG), in which a highly porous, conventional grinding wheel machines the workpiece with very high depths of cut (in some cases, up to even 20 mm) and low feed rates. The process is used in the aerospace and automotive industry in machining difficult-to-cut materials such as superalloys and refers mainly to surface grinding, although can also be used in cylindrical grinding [6, 7]. The second one-pass method – known as traverse contour grinding or continuous path-controlled grinding (CPCG) – is recognised as an alternative to hard turning and consists of using a narrow cylindrical grinding wheel (cBN), which follows the shape of the workpiece [8–10]. The last method involves outside or inside cylindrical traverse grinding with high grinding infeed and electro-corundum grinding wheels, which may be cylindrical or cylindrical with a conic zone for rough grinding, or have a zone-diversified structure [9].

Grinding is a finishing operation, so the influence of elastic deformations of a machine tool–tool–workpiece system is of great importance. Elastic deformations of a workpiece, grinding wheel and machine tool components affect the contact zone between the wheel and the workpiece, thus impacting the shape and dimensional accuracy of the machined part. The types of typical deviations observed after grinding depend on the type of machining process. In the case of traverse grinding of a part mounted between centres, shape deviations depend mostly on the machine tool–tool–workpiece system stiffness and on the accuracy of

setting up the workpiece. In low-stiffness shafts machining, the greatest challenge in achieving the needed accuracy is reducing the cylindricity error resulting from the elastic deformation of the system. Cylindricity errors are dependent on deviations in the straightness of a cylindrical surface [11]. There are two main types of errors produced during traverse grinding. The first one is taper error, which is a result of the elastic deformation of the machine tool centres and is dependent on the difference between the stiffness of a headstock centre and the stiffness of a tailstock centre (Fig. 1a). The second type of error is called barrel error, which results from the elastic deformation of the workpiece (Fig. 1b).

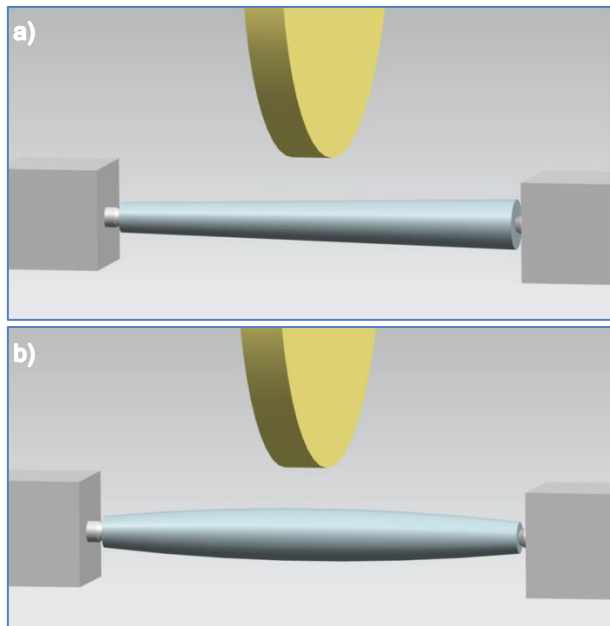


**Fig. 1.** Typical errors in traverse grinding: (a) taper error, (b) barrel error

The values of errors depend on kinematics and the design of the grinding machine, dimensions of the workpiece, technological parameters, among others. The higher the grinding force and the lower the stiffness of the workpiece, the higher the values of the cylindricity error. Thus, the task of machining a low-stiffness workpiece in a single grinding pass proves to be especially difficult [12].

Conventional methods of reducing the shape and size errors of parts machined in traverse grinding aim to reduce the elastic deformation of a machine tool–tool–workpiece system. One way to achieve that goal is by increasing the rigidity of the system by the application of grinding steady rests. However, a proper setting of steady rests on a grinding machine is time-consuming and in many cases requires the skill of an operator. The application of steady rests also involves the risk of damaging the machined surface. The elastic deformation is reduced, but it still can be significant, especially in places distant from the rest and machine centres. One can use a computer numerical controlled CNC-steady rest, but it is expensive and requires changes in the design of a grinding machine. The second way to reduce machining errors is by lowering the grinding force by reducing the values of technological parameters, in particular the axial feed  $f_a$  and the grinding depth  $a_e$ . However, this solution is not very practical due to a significant increase in machining times.

Considering the aforementioned limitations, many researchers tried to develop new strategies in traverse grinding of low-stiffness shafts. Porzycki et al. [13] obtained a significant improvement in the quality of the ground surface, accuracy of the shape of the workpiece and a decrease in the wear of the grinding wheel as a result of the application of the adaptive control system of the axial feed based on the grinding force measurement. Amitay et al. [14] developed an adaptive feed rate control system based on the grinding wheel spindle power signal in order to improve the accuracy of ground workpieces. Gao and Jones [15] designed a test stand for traverse grinding of shafts supported with adaptively controlled steady rests based on the measurement of the diameter of the workpiece during machining. Park et al. [16] developed a model that predicts cylindrical errors resulting from traverse grinding of low-stiffness shafts with steady rests. Choi and Lee [17] proposed a strategy for optimising the position of steady rests to reduce elastic deformation of the workpiece as well as a method for measuring and compensating for thermal deformations during traverse grinding of low-stiffness shafts. Kruszyński and Lajmert [18] developed a system for optimising the traverse grinding process with the use of a neural network. Swic and Taranenko [19] described a method of adaptive control in machining accuracy of axial-symmetrical low-rigidity parts in an elastic-deformable state. The method consisted of additional positive feedback relative to the machining force, and the errors were decreased due to the control of axial feed. Parenti and Bianchi [20] presented a method for improving the surface quality of ground shafts due to the application of a process parameter control system based on the measurement of vibration amplitude and the use of artificial intelligence.

The analysis of the literature revealed that previous studies focused on improving the shape and dimensional accuracy of traverse ground low-stiffness shafts mainly based on the control of technological parameters during the process (resulting in lower machining efficiency), the use of adaptively controlled steady rests or required the use of additional, efficient computational systems and interference in the grinding machine control systems (which limits their use chiefly to laboratory solutions).

## 2. METHOD

In order to achieve accurate and efficient single-pass traverse grinding without the use of steady rests, the following method has been developed. Instead of trying to lower the elastic deformation of the machine tool–tool–workpiece system, a different approach has been undertaken. The method is based on introducing an additional grinding wheel infeed calculated on the basis of the analysis of the cut-layer cross-section and the measurement of the grinding force. During traditional traverse grinding, due to the grinding force exerted on the workpiece, it elastically deforms, resulting in real grinding depth  $a_{er}$  being lower than the set grinding depth  $a_e$  and thus leading to machining errors. In order to obtain low cylindrical deviations, the real grinding depth  $a_{er}$  ought to be as close to the set grinding depth  $a_e$  as possible. The real grinding depth  $a_{er}$  is dependent on many factors, such as stiffness of the machine, workpiece material and its dimensions, type of a grinding wheel and its condition and technological parameters. Many of the factors influencing grinding depth  $a_{er}$  are constant and can be determined before the machining.

Previous research indicates that in traverse grinding of low-stiffness shafts, elements with lowest stiffness, such as workpiece

and machine centres, have a crucial impact on the elastic deformation of the part [10, 21–23]. Depending on the workpiece geometry, they are responsible for up to over 90% of the compliance of the entire system. Taking that into account, one can calculate total elastic deformation at any given place of the workpiece during grinding as a sum of the deformations of machine centres ( $x_1$ ), workpiece deflection ( $x_2$ ) and the deformation of other elements of the system ( $x_3$ ). The elastic deformation of the workpiece due to the deformation of centres can be calculated from the following equation:

$$x_1 = \left(1 - \frac{z}{l}\right)^2 \cdot \frac{F_n}{k_h} + \left(\frac{z}{l}\right)^2 \cdot \frac{F_n}{k_t} \quad (1)$$

where  $z$  is the position of the grinding wheel along the axis of the workpiece,  $F_n$  is the normal component of the grinding force,  $l$  is the length of the workpiece,  $k_h$  is the stiffness of the headstock centre and  $k_t$  is the stiffness of the tailstock centre. For a straight shaft with no steps, the deflection of the workpiece can be calculated as follows:

$$x_2 = \frac{F_n \cdot z^2 \cdot (l - z)^2}{3 \cdot E \cdot I \cdot l} \quad (2)$$

where  $E$  is Young's modulus and  $I$  is the area moment of inertia. The elastic deformation of the remaining components of the system  $x_3$  can be described as follows:

$$x_3 = \frac{F_n}{k_m} \quad (3)$$

where  $k_m$  is the total stiffness of other components of the grinding machine determined experimentally.

The aforementioned equations present simple linear relations between deflections and forces and as such will not describe the deformations resulting from the grinding process as accurately as finite element method (FEM) calculations. However, their simplicity allows for easy and fast calculation and thus may be of use in industrial practice. Considering this, total elastic deformation at any given place of the workpiece during grinding can be calculated from the following equation:

$$x = \left(1 - \frac{z}{l}\right)^2 \cdot \frac{F_n}{k_h} + \left(\frac{z}{l}\right)^2 \cdot \frac{F_n}{k_t} + \frac{F_n \cdot z^2 \cdot (l - z)^2}{3 \cdot E \cdot I \cdot l} + \frac{F_n}{k_m} \quad (4)$$

From the stated relationships, it can be concluded that the deformation of the workpiece during grinding is a function of the normal grinding force component  $F_n$  and the position of the grinding wheel  $z$ . Therefore, the measurement of the normal grinding force  $F_n$  during machining allows for calculating the deformation and for calculating the additional grinding wheel infeed to improve the accuracy of the process. The described method is based on the open-loop control and thus does not require introducing on-line adaptive systems into machine control systems and can be adopted into any CNC-controlled grinding machine equipped with a force sensor. It is based on the measurement of the normal grinding force component  $F_n$  during grinding of a test part with constant grinding wheel infeed  $a_e$ . Then, the additional infeed in each position of the grinding wheel alongside the workpiece is applied when grinding the following parts.

Increasing the grinding depth  $a_e$  results in the increase in the grinding force and, as a consequence, in the increase of the elastic deformation of the workpiece. Therefore, applying the additional infeed based on the elastic deformation calculated from the measured force would decrease the machining errors, but to

achieve the lowest values of deviations, the additional deformation ought to be considered.

Fig. 2 presents a simplified view of the ground layer cross-section depending on the grinding wheel infeed.

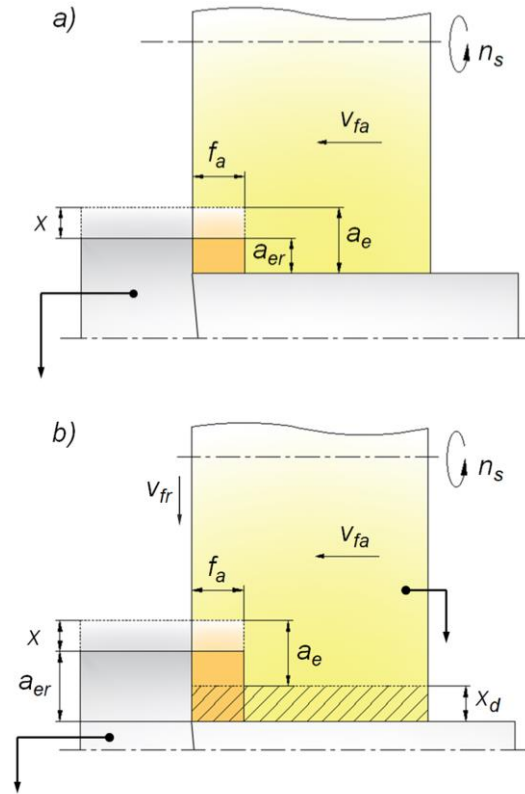


Fig. 2. A view of the ground layer cross-section: (a) with constant grinding wheel infeed, (b) with additional grinding wheel infeed

Considering this, a relationship describing the real grinding depth can be formulated as follows:

$$a_{er} = a_e - x + x_d \quad (5)$$

where  $x_d$  is the value of the additional infeed at a given grinding wheel position. As follows from Eq. (5), the real grinding depth  $a_{er}$  will be equal to the set grinding depth  $a_e$  when the value of the total elastic deformation  $x$  is equal to the value of the additional grinding wheel infeed  $x_d$ . Therefore, the value of the additional infeed of the grinding wheel at any given place during machining can be determined from the following relationship:

$$x_d = F_n \left[ \left(1 - \frac{z}{l}\right)^2 \cdot \frac{1}{k_h} + \left(\frac{z}{l}\right)^2 \cdot \frac{1}{k_t} + \frac{z^2 \cdot (l - z)^2}{3 \cdot E \cdot I \cdot l} + \frac{1}{k_m} \right] \quad (6)$$

Considering this, in order to calculate the additional infeed of the grinding wheel, it is necessary to determine, besides geometrical and material parameters of the workpiece and stiffness coefficients of the machine, the value of the normal grinding force  $F_n$  applied to the workpiece when grinding with  $a_e = a_{er}$ . Thus, in the presented method, it is necessary to grind a test part with a constant grinding wheel infeed in order to measure the normal grinding force value. The method is best suited for parts with low variations in machining allowance because adopted equations assume the allowance is constant, and thus, any significant change in the shaft diameter between parts will influence the accuracy of produced parts. In addition, due to the wear of a grinding wheel, the grinding force should be measured during each grinding pass to

recalculate the values of the infeed and thus to ensure high accuracy for all the parts.

In addition, in traverse grinding, due to the abrupt change in the machining load at the beginning and at the end of each grinding pass, cylindrical deviations, which often surpass the deviations resulting from the deflection of a workpiece, tend to occur. In order to reduce these errors, the presented method involves a strategy of gradual entry and exit of the grinding wheel from the workpiece, thus allowing to avoid sudden increases and decreases in the machining load. The strategy consisted of moving the grinding wheel linearly in both X and Z axes from the depth of  $a_e = 0 \mu\text{m}$  up to the set  $a_e$  at the grinding length that was equal to a quarter of the grinding wheel width.

### 3. EXPERIMENTAL SETUP

In order to check the effectiveness of the proposed method, experimental tests were performed. The experimental setup was designed based on a three-axis CNC cylindrical grinding machine by Geibel & Hotz (Fig. 3). The measurement of the grinding force was conducted with two dynamometers of type 9601A31 by Kistler. The signal from the dynamometers was amplified and registered with an A/D converter type NI USB-6009 by National Instruments and a computer equipped with LabVIEW SignalExpress software.

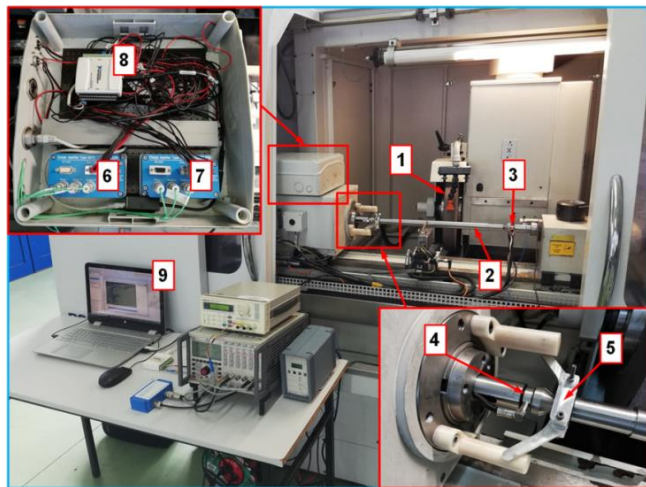


Fig. 3. Test stand: 1 – grinding wheel; 2 – workpiece; 3,4 – dynamometers; 5 – grinding carrier; 6,7 – signal amplifiers; 8 – A/D converter; 9 – computer with LabVIEW SignalExpress software

The measurement of the accuracy of the grinded workpiece was conducted on the grinding machine, with the use of an inductive sensor type GT 21 by TESA (Fig. 4). The sensor mounted on the grinding wheel spindle unit allowed recording the profiles of grinded shafts. The cylindricity error  $\Delta C$  was calculated as a difference between the maximum  $\Delta r_{wmax}$  and minimum  $\Delta r_{wmin}$  values recorded by the sensor during the measurement. The measurement of the diameter of a workpiece was conducted with the Micromar 8 control gauge by Marposs. Such a measuring setup was investigated in previous works and proved to be accurate [24]. The values of the stiffness coefficients were determined experimentally by loading the respective part of the machine and measuring the resultant deflection with the inductive sensor. The

determined values were as follows:  $k_h = 7.12 \text{ kN/mm}$ ,  $k_t = 5.03 \text{ kN/mm}$  and  $k_m = 21.43 \text{ kN/mm}$ .

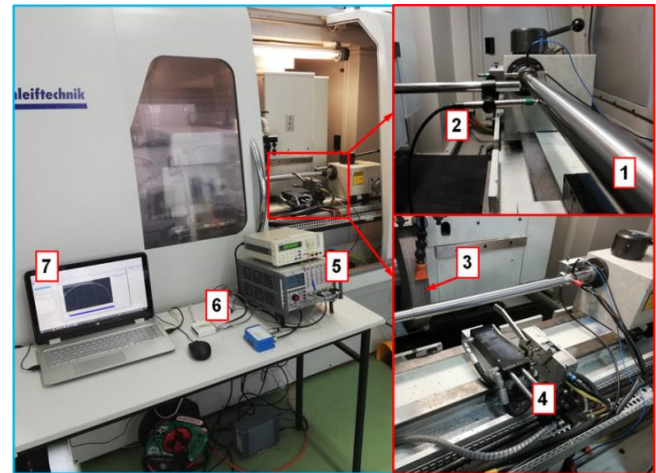


Fig. 4. Test stand: 1 – workpiece; 2 – inductive sensor; 3 – grinding wheel; 4 – control gauge; 5 – amplifier; 6 – A/D converter; 7 – computer

The M60H12VEPI electro-corundum grinding wheel by Andre Abrasives was used in the tests. The width of the grinding wheel was equal to  $b_s = 50 \text{ mm}$ . The workpieces in the shape of straight shafts with the length of  $l = 500 \text{ mm}$  and the diameter of  $d_w = 30 \text{ mm}$  were machined from the 100Cr6 steel and underwent thermal treatment in order to achieve a hardness of approx. 60 HRC. On both sides of the shafts, there was a step with a diameter of 25 mm so as to enable entry and exit of the grinding wheel, as well as to allow mounting of the grinding carrier. Thus, the grinding length was equal to  $l_s = 375 \text{ mm}$ . The workpieces were grinded in a single pass of a grinding wheel with constant infeed and with the variable infeed. The direction of grinding was from the headstock to the tailstock. After each machining pass, the grinding wheel was dressed in order to restore its cutting capabilities. For the experimental tests, such a range of technological parameters was assumed, which allowed utilising the capabilities of the grinding machine and simultaneously did not cause the loss of stability of the machining. The technological parameters are presented in Table 1.

Tab. 1. Values of set technological parameters for the grinding tests

Technological parameter	Value
Grinding wheel speed $v_s$ (m/s)	35
Grinding wheel infeed $a_e$ ( $\mu\text{m}$ )	20, 40, 60, 80, 100, 120
Grinding feed $f_a$ (mm/obr)	1
Workpiece speed $v_w$ (m/s)	0.44
Dressing infeed $a_{ed}$ ( $\mu\text{m}$ )	10
Dressing feed $f_{ad}$ (mm/obr)	0.1

### 4. RESULTS

Fig. 5 presents recorded deviations of the grinded workpiece profiles after tests with the variable infeed and with the constant infeed.

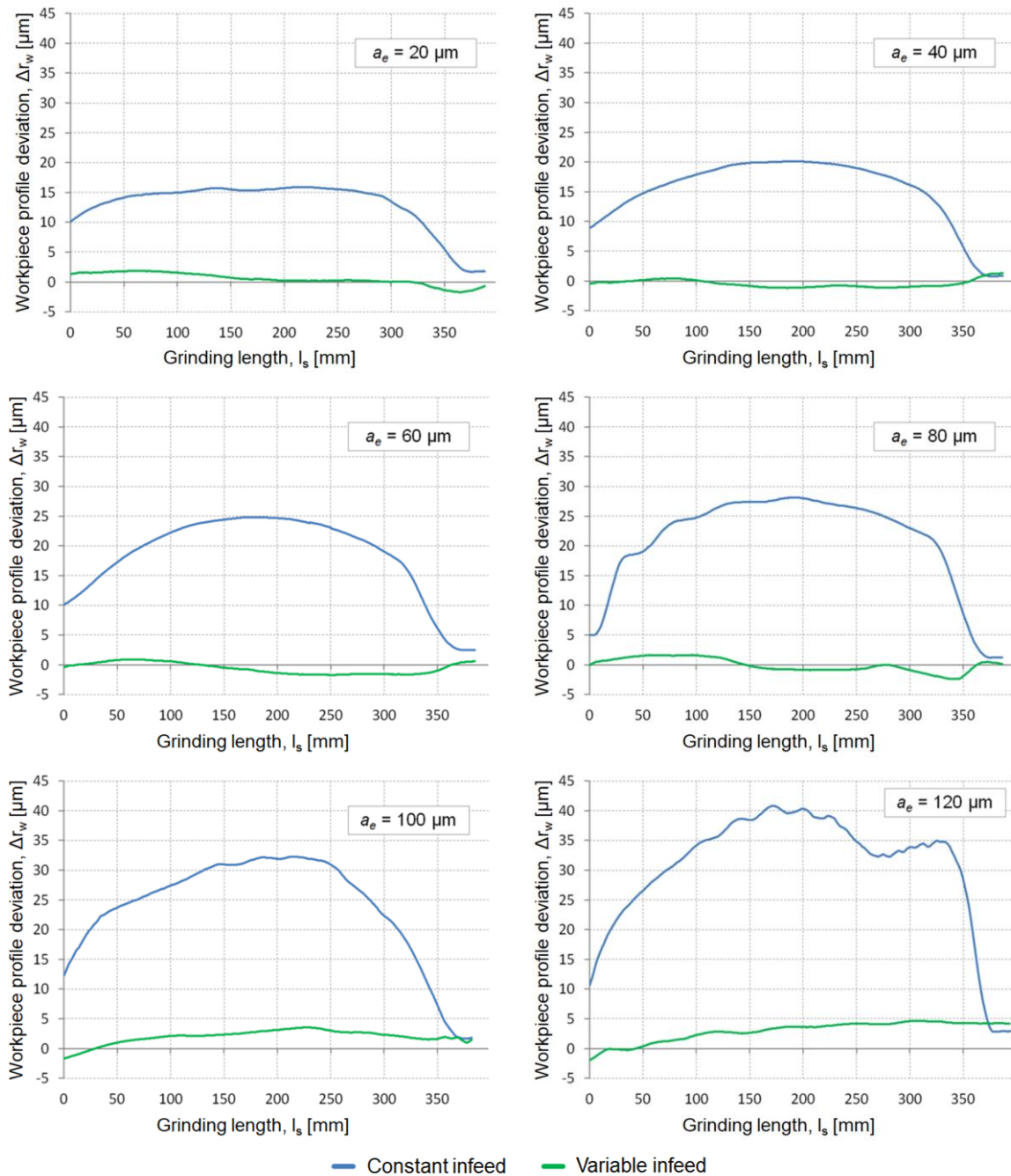


Fig. 5. Deviations of the grinded workpiece profiles

Analysing the deviations recorded after grinding tests with constant grinding infeed, one can observe that with the increase in the grinding length, due to elastic deformation of the machining system, the values of the deviations increase until they reach a maximum, which is situated usually near the lowest stiffness point of the system. Then, the deviations gradually decrease until the grinding wheel exits the workpiece, where a sudden decrease in errors can be observed due to the reduction in elastic deformations of the system. The difference in the rate of the deviation increase and decrease results from the difference in the stiffness of the machine tool centres.

The analysis of the presented graphs leads to the conclusion that grinding with variable infeed can significantly decrease the deviations of the grinded profiles in the tested range of the grinding depths. For grinding with constant infeed, the biggest variations in recorded deviations were observed at the start and the

end of the grinding, especially with lower grinding depths, where the deflection of the workpiece is comparably low. The increase in grinding depth resulted in an increase in the strain of the machine tool–tool–workpiece system and thus in the increase in recorded deviations. The local decrease in deviation values of the workpiece grinded with  $a_e = 120 \mu\text{m}$  indicates the loss of stability of the machining. For the selected geometry of shafts, trying to grind with  $a_e > 120$  resulted in the sudden increase in forces and vibrations, resulting in chipping of the grinding wheel. On the other hand, the deviations of the grinded profiles recorded after grinding with variable infeed were close to linear. For the grinding depths of  $a_e = 100 \mu\text{m}$  and  $a_e = 120 \mu\text{m}$ , one can observe an increase in deviation values with an increase in grinding length. For other grinding depths, the errors did not show a clear tendency of changes. For all the grinding tests with variable infeed, the measured deviations were in the range of  $-3 \mu\text{m}$  to  $+5 \mu\text{m}$ .

In addition, the local decrease in deviations recorded after grinding with a constant infeed of  $a_e = 120 \mu\text{m}$  indicate the loss of stability of the machining. On the other hand, when grinding with the additional infeed, the loss of stability was not observed.

Fig. 6a presents the values of calculated cylindricity errors. Fig. 6b presents the maximum dimensional error recorded after grinding. As can be seen from the graph, for the tests with constant grinding infeed, there was a monotonous and almost linear dependence between the grinding depth and cylindricity deviation. For the tests conducted with variable infeed, the recorded values of cylindrical deviation were equal to approximately  $5 \mu\text{m}$  for all the analysed grinding depths. The higher the set grinding depth, the higher the obtained deviations.

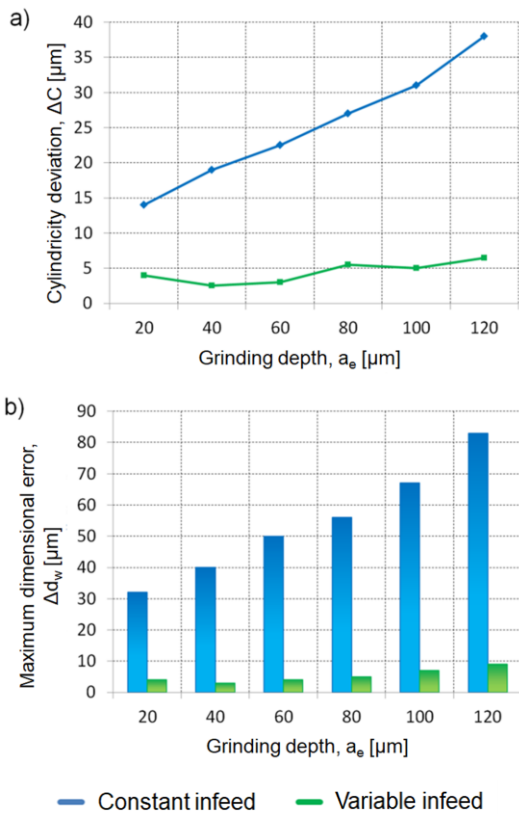


Fig. 6. Deviations of the workpieces grinded with various set grinding depths: (a) cylindricity error, (b) maximum dimensional error

The analysis of the recorded cylindricity deviations leads to a conclusion that applying the variable infeed can decrease the cylindricity deviations up to 87%, on average approx. 82%. In addition, the maximum dimensional error was reduced by approx. 90% in comparison to grinding with constant grinding infeed.

Fig. 7 presents the values of the normal component of grinding force recorded during grinding tests.

As can be observed from the presented graphs, the use of the additional infeed resulted in the increase in the normal grinding force component for all set grinding depths. The values of force measured when grinding with constant infeed increase with the increase in grinding time due to the wear of the grinding wheel and the increase in the system stiffness resulting from the grinding wheel getting closer to the tailstock centre. On the other hand, the course of  $F_n$  changes recorded during grinding indicates stabilisation of its value. During grinding with variable infeed, the average values of the normal cutting force component were higher than

those when grinding with constant infeed, with an increase of approximately 11%.

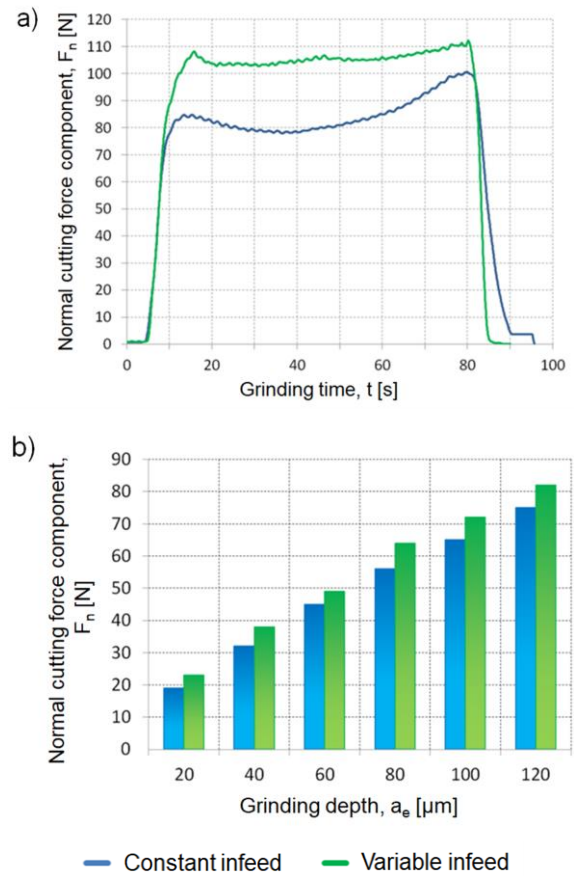


Fig. 7. Normal grinding force component: (a) courses of changes (b) average values

One of the most important indicators of the effectiveness of the grinding process is the quality of the manufactured surface. In order to assess the influence of the proposed method on the surface roughness of grinded parts,  $R_a$  surface roughness parameter was measured after each grinding test. Fig. 8 presents the results of the measurements conducted at the start, in the middle and at the end of the workpiece.

Analysing the roughness of the parts, one can observe that the higher the grinding depth, the lower the quality of the manufactured surface, which is true for both grinding with constant and with variable infeed, especially at the beginning and at the end of the workpiece. At the beginning, in the case of grinding with constant infeed, every increase in the grinding depth  $a_e$  of  $20 \mu\text{m}$  results in a significant increase in  $R_a$  parameter, approximately 13%. On the other hand, surface roughness measured at the start of the part grinded with variable infeed did not show such clear increasing tendency and was equal approx.  $R_a 0.2\text{--}0.25 \mu\text{m}$  for all the grinding depths. A significant difference between surface roughness measured at the end of the workpiece after grinding with constant and variable infeed was observed as well. The values of surface roughness  $R_a$  decreased on average by approximately 26% when grinding with variable infeed. However, increasing the infeed during grinding did not result in a significant increase in  $R_a$  parameters measured in the middle of the workpiece (on average approx. 4% increase). No significant increase

in surface roughness of grinded parts was measured in the middle of the workpiece, even though the machining load was higher, which may result from the higher stability of the machining with the additional grinding infeed. The reduction in surface roughness  $R_a$  measured at the beginning and at the end of the workpiece may result from the gradual entry and exit of the grinding wheel, which allowed for reducing the loading impact and thus improving the quality of the surface at those parts of the workpiece.

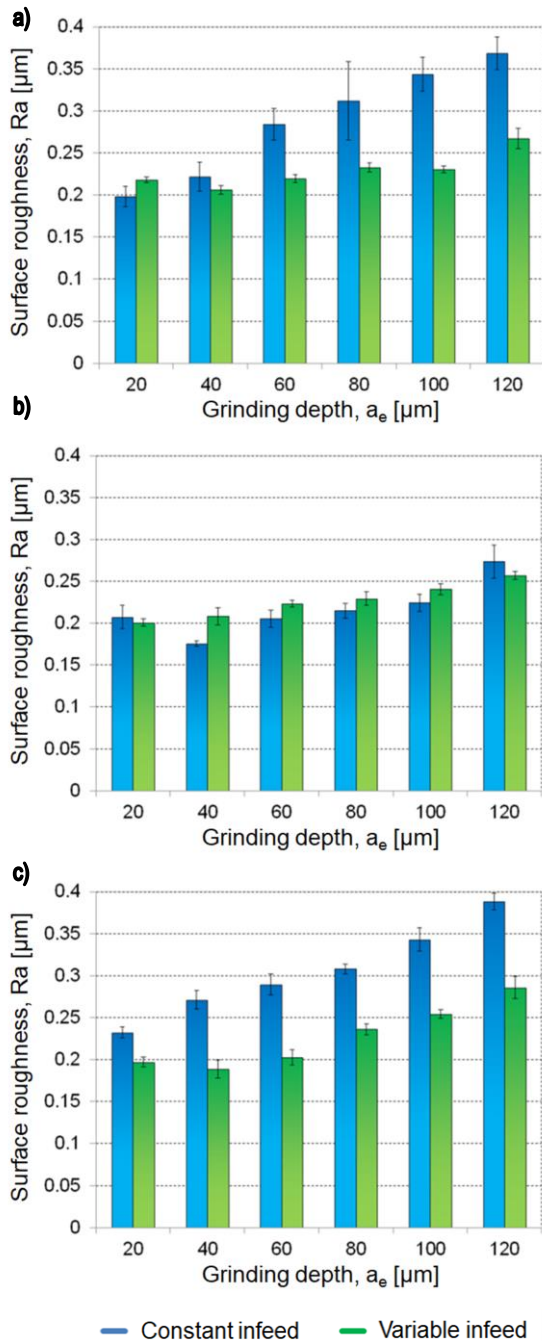


Fig. 8. Surface roughness  $R_a$  of the test parts: (a) at the beginning (b) in the middle (c) at the end

### 5. CONCLUSIONS

The article presents a method of increasing the shape and dimensional accuracy of low-stiffness shafts manufactured in a

single pass of a grinding wheel in traverse grinding. The method consisted of applying additional infeed calculated in each position of the grinding wheel based on the measurement of the normal component of the grinding force. In order to prove its effectiveness, experimental tests were conducted. Low-stiffness shafts were grinded in a single pass of a grinding wheel with constant and variable infeed. The results showed that grinding with the use of the proposed method can significantly improve the quality of manufactured workpieces. For the analysed range of set grinding depths, grinding with variable infeed allowed reducing the cylindricity deviations to a few micrometres, which constitutes a decrease of, on average, approximately 82%. In addition, the maximum dimensional error was reduced by approx. 90% in comparison to grinding with constant grinding infeed. Grinding tests with the use of the method resulted in increasing the normal grinding force component, on average approximately by 11%. However, the increased load did not correspond with the increase in surface roughness. The measurements of  $R_a$  surface roughness parameter showed that at the beginning and at the end of the workpiece, grinding with variable infeed improved the quality of the surface. Thus, the presented method may constitute a viable option when grinding low-stiffness shafts in a single pass of a grinding wheel without the use of steady rests.

### REFERENCES

- Han X., Wu T. Analysis of acoustic emission in precision and high-efficiency grinding technology. *Int J Adv Manuf Tech.* 2013; 67(9):1997-2006.
- Ocoś K. Characteristics of development trends in grinding with grinding wheels. *Materials of XXIII Scientific Abrasive Conference 2000*; 13-62.
- Kopac J., Krajnik P. High-performance grinding – A review. *J Mater Process Tech.* 2006;175:278-284.
- Klocke F., Barth S., Mattfeld P. High Performance Grinding. *Procedia CIRP.* 2016;46:266-271.
- Klocke F., Soo L., Karpuschewski B., Webster J., Novovic D., Elfizy A., Axinte D., Tönissen S. Abrasive machining of advanced aerospace alloys and composites. *CIRP Annals – Manufacturing Technology.* 2015;64(2):581-604.
- Kalchenko V., Pogiba N., Kalchenko D. Determination of Cutting Force Components in Creep-Feed Grinding of Revolution Surfaces Using an Oriented Elbor Wheel. *J Superhard Mater.* 2012;34(2): 118-130.
- Żyłka Ł., Babiarz R. Dressing process in the grinding of aerospace blade root. *J Mech Sci Technol.* 2017;31(9): 4411-4417.
- Webster J., Tricard M. Innovations in Abrasive Products for Precision Grinding. *CIRP Annals.* 2004;53(2):597-617.
- Nadolny K. A review on single-pass grinding processes. *J Cent South Univ.* 2013;20:1502-1509.
- Burek J., Sułkowicz P., Babiarz R., Płodzień M. Cylindrical Continuous Path Controlled Grinding with Profile Grinding Wheel Type 1F1. *Reszow University of Technology Scientific Letters, Mechanics.* 2017;89(4):449-456.
- Marinescu I. D., Hitchiner M. P., Uhlmann E., Rowe W. B., Inasaki I. *Handbook of Machining with Grinding Wheels.* CRC Press, 2016.
- Urbicain G., Olvera D., Fernandez A., Rodriguez L., Tabernero L.N. Stability Lobes in Turning of Low Rigidity Components. *Adv Mat Res.* 2012;498:576-585.
- Porzycki J., Batsch A., Ocoś K. A two-parameter adaptive control system for the traverse cylindrical grinding process. *IFAC Proceedings Volumes.* 1980;13(10):151-154.
- Amitay G., Malkin S., Koren Y. Adaptive Control Optimization of Grinding. *J Eng Ind.* 1981;103(1):103-108.

15. Gao Y., Jones B. Control of the traverse grinding process using dynamically active workpiece steadies. . *Int J Mach Tool Manu.* 1993;33(2):231-244.
16. Park C., Kim D., Lee S. Shape prediction during the cylindrical traverse grinding of a slender workpiece. *J Mater Process Tech.* 1999;88:23-32.
17. Choi H., Lee S. Machining error compensation of external cylindrical grinding using thermally actuated rest. *Mechatronics.* 2002;12: 643-656.
18. Kruszyński B., Lajmert W. An intelligent system for online optimization of the cylindrical traverse grinding operation. *Int J Eng Manu.* 2006;3:355-363.
19. Świć A., Taranenko W. Adaptive control of machining accuracy of axial – symmetrical lowrigidity parts in elastic – deformable state. *Maintenance and Reliability.* 2012;3:215-221.
20. Parenti P., Bianchi G. Model-based adaptive process control for surface finish improvement in traverse grinding. *Mechatronics.* 2016;36:97-111.
21. Saljé E., Mushardt H. Aufbau einer Optimierregelung für einen mehrstufigen Schleifprozess. *Werkstattstechnik.* 1975;65:335-338.
22. Burek J. Stabilization of normal grinding force component in multi-stage plunge grinding. PhD thesis (Rzeszow University of Technology). 1985.
23. Onishi T., Kodani T., Ohashi K., Sakakura M., Tsukamoto S. Study on the Shape Error in the Cylindrical Traverse Grinding of a Workpiece with High Aspect Ratio. *Adv Mat Res.* 2014;10(17):78-81.
24. Burek J., Sułkowicz P., Babiarz R. Cylindricity error measurement and compensation in traverse grinding of low-stiffness shafts. *Mechanik.* 2018;91(11):970-972.

Paweł Sułkowicz:  <https://orcid.org/0000-0003-4604-7683>

Robert Babiarz:  <https://orcid.org/0000-0002-3418-6670>

Jan Burek:  <https://orcid.org/0000-0003-2664-5248>

Jarosław Buk:  <https://orcid.org/0000-0002-8997-4877>

Kamil Gancarczyk:  <https://orcid.org/0000-0002-5938-6636>